Two-color multi-section quantum dot distributed feedback laser

Nader A. Naderi,[1,*] Frédéric Grillot,[2] Kai Yang,[1] Jeremy B. Wright,[3] Aaron Gin,[3] and Luke F. Lester[1]

[1]*Center for High Technology Materials, University of New Mexico, 1313 Goddard SE, Albuquerque, New Mexico 87106, USA*
[2]*Université Européenne de Bretagne, INSA, CNRS- Laboratoire FOTON, 20 avenue des buttesde Coesmes, 35708 Rennes, Cedex 7, France*
[3]*Sandia National Laboratories, Center for Integrated Nanotechnologies, 1101 Eubank SE, Albuquerque, New Mexico 87185, USA*
*nader@unm.edu

Abstract: A dual-wavelength emission source is realized by asymmetrically pumping a two-section quantum-dot distributed feedback laser. It is found that under asymmetric bias conditions, the powers between the ground-state and excited-state modes of the two-section device can be equalized, which is mainly attributed to the unique carrier dynamics of the quantum-dot gain medium. As a result, a two-color emission with an 8-THz frequency difference is realized that has potential as a compact THz source. It is also shown that the combination of significant inhomogeneous broadening and excited-state coupled mode operation allows the manipulation of the quantum-dot states through external optical stabilization.

OCIS codes: (140.3490) Distributed-feedback lasers; (140.5960) Semiconductor lasers; (250.5590) Quantum-well, -wire and -dot devices; (300.6495) Spectroscopy, terahertz; (060.5625) Radio frequency photonics.

References and links

1. M. Koch, "Terahertz Communications: A 2020 Vision," in *Terahertz Frequency Detection and Identification of Materials and Objects*, R. E. Miles, X. –C. Zhang, H. Eisele, A. Krotkus, eds. (Springer, New York, 2007).
2. P. H. Siegel, "Terahertz technology in biology and medicine," IEEE Trans. Microw. Theory Tech. 52(10), 2438–2447 (2004).
3. P. F. Taday, "Applications of terahertz spectroscopy to pharmaceutical sciences," Philos. Transact. A Math. Phys. Eng. Sci. 362(1815), 351–363, discussion 363–364 (2004).
4. S. Wang, B. Ferguson, D. Abbott, and X.-C. Zhang, "T-ray imaging and tomography," J. Biol. Phys. 29(2/3), 247–256 (2003).
5. C. Baker, T. Lo, W. R. Tribe, B. E. Cole, M. R. Hogbin, and M. C. Kemp, "Detection of concealed explosives at a distance using terahertz technology," in *Proceedings of IEEE on T-Ray Imaging, Sensing, and Retection*, (Institute of Electrical and Electronics Engineers, New York, 2007), pp. 1559–1565.
6. D. Saeedkia, and S. Safavi-Naeini, "Terahertz photonics: optoelectronic techniques for generation and detection of terahertz waves," J. Lightwave Technol. 26(15), 2409–2423 (2008).
7. A. Klehr, J. Fricke, A. Knauer, G. Erbert, M. Walther, R. Wilk, M. Mikulics, and M. Koch, "High-power monolithic two-mode DFB laser diodes for the generation of THz radiation," IEEE J. Sel. Top. Quantum Electron. 14(2), 289–294 (2008).
8. M. Tani, O. Morikawa, S. Matsuura, and M. Hangyo, "Generation of terahertz radiation by photomixing with dual- and multiple-mode lasers," Semicond. Sci. Technol. 20(7), S151–S163 (2005).
9. M. Naftaly, M. R. Stone, A. Malcoci, R. E. Miles, and I. Camara Mayorga, "Generation of CW terahertz radiation using two-colour laser with Fabry-Perot etalon," Electron. Lett. 41(3), 128–129 (2005).
10. L. F. Lester, K. C. Hwang, P. Ho, J. Mazurowski, J. M. Ballingall, J. Sutliff, S. Gupta, J. Whitaker, and S. L. Williamson, "Ultra-fast long-wavelength photodetectors fabricated on low-temperature InGaAs on GaAs," IEEE Photon. Technol. Lett. 5(5), 511–514 (1993).
11. E. R. Brown, "THz generation by photomixing in ultrafast photoconductors," Int. J. High Speed Electron. Syst. 13(2), 497–545 (2003).
12. K. A. McIntosh, E. R. Brown, K. B. Nichols, O. B. McMahon, W. F. DiNatale, and T. M. Lyszczarz, "Terahertz measurements of resonant planar antennas coupled to low-temperature-grown GaAs photomixers," Appl. Phys. Lett. 69(24), 3632–3634 (1996).

#136197 - $15.00 USD Received 6 Oct 2010; revised 26 Nov 2010; accepted 2 Dec 2010; published 8 Dec 2010

13. J. C. Pearson, K. A. McIntosh, and S. Verghese, *Long-Wavelength Infrared Semiconductor Lasers* (John Wiley & Sons, 2005), Chap. 7.
14. C.-L. Wang, and C.-L. Pan, "Tunable multiterahertz beat signal generation from a two-wavelength laser-diode array," Opt. Lett. 20(11), 1292–1294 (1995).
15. P. Pellandini, R. P. Stanley, R. Houdrè, U. Oesterle, M. Ilegems, and C. Weisbuch, "Dual-wavelength laser emission from a coupled semiconductor microcavity," Appl. Phys. Lett. 71(7), 864–866 (1997).
16. S. Hoffmann, M. Hofmann, E. Bründermann, M. Havenith, M. Matus, J. V. Moloney, A. S. Moskalenko, M. Kira, S. W. Koch, S. Saito, and K. Sakai, "Fourwave mixing and direct terahertz emission with two-color semiconductor lasers," Appl. Phys. Lett. 84(18), 3585–3587 (2004).
17. S. Zolotovskaya, V. I. Smirnov, G. B. Venus, L. B. Glebov, and E. U. Rafailov, "Two-color output from InGaAs laser with multiplexed reflective Bragg mirror," IEEE Photon. Technol. Lett. 21(15), 1093–1095 (2009).
18. M. Hyodo, M. Tani, S. Matsuura, N. Onodera, and K. Sakai, "Generation of millimeter-wave radiation using a dual-longitudinal-mode microchip laser," Electron. Lett. 32(17), 1589–1591 (1996).
19. P. Bhattacharya, D. Klotzkin, O. Qasaimeh, W. Zhou, S. Krishna, and D. Zhu, "High-speed modulation and switching characteristics of In(Ga)As–Al(Ga)As self-organized quantum-dot lasers," IEEE J. Sel. Top. Quantum Electron. 6(3), 426–438 (2000).
20. A. Stintz, G. T. Liu, H. Li, L. F. Lester, and K. J. Malloy, "Low-threshold current density 1.3-μm InAs quantum-dot lasers with the dots-in-a-well (DWELL) structure," IEEE Photon. Technol. Lett. 12(6), 591–593 (2000).
21. T. C. Newell, D. J. Bossert, A. Stintz, B. Fuchs, K. J. Malloy, and L. F. Lester, "Gain and linewidth enhancement factor in InAs quantum-dot laser diodes," IEEE Photon. Technol. Lett. 11(12), 1527–1529 (1999).
22. C. Y. Jin, H. Y. Liu, T. J. Badcock, K. M. Groom, M. Gutiérrez, R. Royce, M. Hopkinson, and D. J. Mowbray, "High-performance 1.3 [micro sign]m InAs/GaAs quantum-dot lasers with low threshold current and negative characteristic temperature," IEE Proc., Optoelectron. 153(6), 280–283 (2006).
23. A. Markus, J. X. Chen, C. Paranthoën, A. Fiore, C. Platz, and O. Gauthier-Lafaye, "Simultaneous two-state lasing in quantum-dot lasers," Appl. Phys. Lett. 82(12), 1818–1820 (2003).
24. M. A. Cataluna, D. I. Nikitichev, S. Mikroulis, H. Simos, C. Simos, C. Mesaritakis, D. Syvridis, I. Krestnikov, D. Livshits, and E. U. Rafailov, "Dual-wavelength mode-locked quantum-dot laser, via ground and excited state transitions: experimental and theoretical investigation," Opt. Express 18(12), 12832–12838 (2010).
25. M. Kamp, J. Hofmann, F. Schafer, M. Reinhard, M. Fischer, T. Bleuel, J. P. Reithmaier, and A. Forchel, "Lateral coupling -a material independent way to complex coupled DFB lasers," Opt. Mater. 17(1-2), 19–25 (2001).
26. H. Su, and L. F. Lester, "Dynamic properties of quantum dot distributed feedback lasers: high speed, linewidth and chirp," J. Phys. D Appl. Phys. 38(13), 2112–2118 (2005).
27. T. Nakura, and Y. Nakano, "LAPAREX-An automatic parameter extraction program for gain- and index-coupled distributed feedback semiconductor lasers, and its application to observation of changing coupling coefficients with currents," IEICE Trans. Electron. 83(3), 488–495 (2000).
28. P. Bhattacharya, "Lasers: structures and properties" in *Semiconductor Optoelectronic Devices*, E. Svendsen, R. Kernan, P. Daly, eds. (Prentice Hall, Upper saddle river, NJ, 1994).
29. F. Grillot, K. Veselinov, M. Gioannini, I. Montrosset, J. Even, R. Piron, E. Homeyer, and S. Loualiche, "Spectral analysis of 1.55-μm InAs/InP (113)B quantum-dot lasers based on a multipopulation rate equations model," IEEE J. Quantum Electron. 45(7), 872–878 (2009).
30. C. Mesaritakis, C. Simos, H. Simos, S. Mikroulis, I. Krestnikov, E. Roditi, and D. Syvridis, "Effect of optical feedback to the ground and excited state emission of a passively mode locked quantum dot laser," Appl. Phys. Lett. 97(6), 061114 (2010).
31. F. Grillot, N. A. Naderi, M. Pochet, C.-Y. Lin, and L. F. Lester, "Variation of the feedback sensitivity in a 1.55μm InAs/InP quantum-dash Fabry-Perot semiconductor laser," Appl. Phys. Lett. 93(19), 191108 (2008).
32. F. Grillot, N. A. Naderi, M. Pochet, C.-Y. Lin, P. Besnard, and L. F. Lester, "Tuning of the critical feedback level in 1.55-μm quantum dash semiconductor laser diodes," IET Optoelectron. 3(6), 242–247 (2009).

1. Introduction

Terahertz (THz) technology has a wide variety of applications in fields as diverse as next generation computing and communications technologies, medical and pharmaceutical fields as well as basic material science and homeland security [1–5]. Recently, significant progress has been made in the field of THz source generation, which has created engineering opportunities that exploit this new technology [6]. Specifically, there has been interest in the development of THz optoelectronic sources since their electronic addressability and tunability would make them easier to operate [7]. For this particular source, two coherently interfering optical modes are typically generated by two single-mode lasers, and the light is absorbed in an ultrafast photoconductive semiconductor [8–10]. This process creates time varying electron and hole densities that under the influence of an applied electric field are accelerated and generate a THz wave that is equal to the difference frequency between the two optical modes [11]. Among other uses, such THz signals can be coupled to a radiating antenna for

#136197 - $15.00 USD Received 6 Oct 2010; revised 26 Nov 2010; accepted 2 Dec 2010; published 8 Dec 2010

transmission [12], and the frequency of the THz signal can be changed by varying the wavelengths of the optical modes. In order to tune and stabilize the frequency output of the semiconductor lasers, an external cavity is commonly used that requires a relatively bulky opto-mechanical design. Thus, it is highly desirable to develop a THz signal source that is more compact and inexpensive to fabricate. One possible approach is to use a dual-mode semiconductor laser that features a device with two longitudinal modes simultaneously emitting at two different frequencies from a single or combined laser cavity [13]. The use of the dual-mode laser has the advantage of being free of optical alignment issues since there is no need to align two laser beams, which is critical for photomixing efficiency. Several optical cavity approaches have been studied that achieve simultaneous two-color generation from a compact, monolithic system [14–17]. The dual-mode laser source for THz generation has been previously studied in bulk and Quantum-Well (QW) semiconductor lasers [15–18], but very little is known about the behavior of nanostructured active regions in these types of devices.

Compared to QW and bulk materials, nanostructures such as Quantum-Dots (QDs) are known to have superior characteristics due to their ultrafast carrier dynamics, ultralow threshold current density, reduced linewidth enhancement factor, and improved temperature characteristics [19–22]. Simultaneous ground-state (GS) and excited-state (ES) with *multi-mode* emissions have been previously observed in QD material when increasing the bias current well above the threshold [23,24]. The technical approach described in this paper simultaneously addresses the need for compact size, low fabrication cost, and high performance by concurrently generating two *single-mode* emission peaks–one line from the GS and the other from the ES of the laser device. The laser source used in this investigation is a two-section Laterally Loss-Coupled (LLC) Distributed Feedback (DFB) laser in which the Bragg grating is coupled only to the QD ES. Two-color operation is realized through simultaneous GS emission that is uncoupled to the Bragg grating due to inhomogeneous broadening in the QD active medium.

In order to accurately characterize the performance of the DFB device under investigation, the values of the index and gain coupling coefficients are calculated by using the numerical least-squares-fitting of the sub-threshold spectra. The two-color emission is then demonstrated in the DFB device by using either (1) an asymmetric bias configuration or (2) an external optical feedback stabilization under uniform pumping conditions. Finally, it is suggested that the combination of both techniques while taking the advantage of unique characteristics of the QD gain media can further optimize the performance of the two-section QD DFB laser as a continuous-wave (CW) THz source by purifying and stabilizing the two-color operation in a well-controlled manner.

2. Device structure, fabrication and characterizations

The epitaxial structure and two-section waveguide design are schematically shown in Fig. 1(a). The InAs/InGaAs dots-in-a-well (DWELL) laser structure was grown by elemental source molecular beam epitaxy on a (001) n^+-GaAs substrate. The active region consists of six stacks of InAs QDs embedded in $In_{0.15}Ga_{0.85}As$ QWs each separated by undoped GaAs barrier layers. The upper and lower cladding layers were 1.30 μm thick $Al_{0.66}Ga_{0.34}As$. Room temperature photoluminescence (PL) measurements show that the QD material has a nominal GS lasing around 1240 nm. The device fabrication starts with formation of 3 μm wide ridge-waveguides (RWG), etched by the inductively coupled plasma (ICP) etching technique. As illustrated in Fig. 1(b), the two-section LLC-DFB laser bars were fabricated by patterning 100 nm wide lateral absorptive chromium grating lines adjacent to 3 μm wide ridges using a JEOL JBX-6300FS electron-beam lithography system followed by metal evaporation and liftoff.

#136197 - $15.00 USD Received 6 Oct 2010; revised 26 Nov 2010; accepted 2 Dec 2010; published 8 Dec 2010

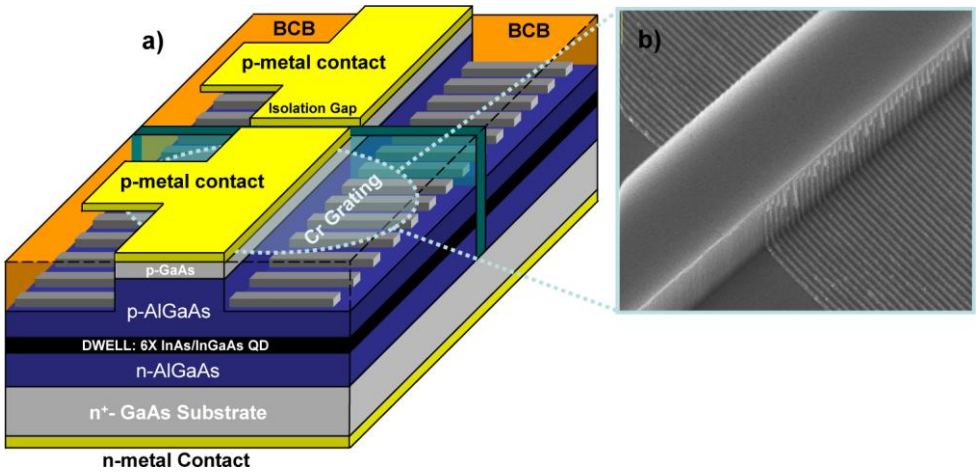

Fig. 1. (a) Oblique schematic view of the epitaxial layers and two-section cavity structure of the InAs QD LLC-DFB laser. (b) Oblique SEM image of the 100 nm wide chromium grating lines adjacent to the ridge waveguide processed by electron-beam lithography and metal evaporation.

The first order metal grating pitch size is around 190 nm. It is important to note that the LLC–DFB structure has the advantages of a gain-coupled device without requiring re-growth [25]. After surface planarization using benzocyclobutene (BCB), the Ti/Pt/Au layers were deposited to form the p-metal contact. The electrical isolation between the two 500 μm long sections was provided by proton implantation with an isolation resistance of >10 MΩ. Finally the substrate was lapped and polished, and a Ge/Au/Ni/Au n-metal contact layer was deposited and annealed at ~380 °C. The two-section QD DFB laser was cleaved at both facets and has a total cavity length of 1 mm.

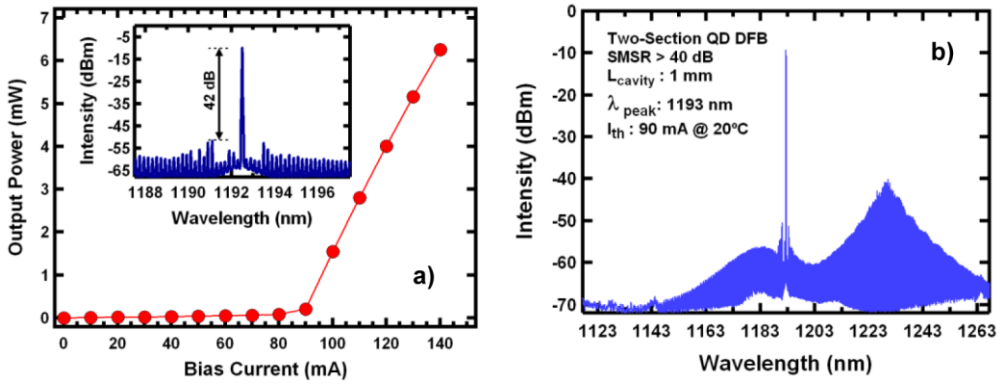

Fig. 2. (a) Room temperature Light-Current characteristics of the two-section QD DFB laser. The inset figure shows the optical spectrum of the solitary laser at 110 mA with a side-mode suppression ratio of > 40 dB. (b) Broad optical spectrum of the two-section DFB laser at 110 mA indicating the existence of the ES and GS peaks under uniform pumping condition.

Figure 2(a) represents the light-current characteristic, L(I), measured under uniform pumping and at room temperature. When the two laser sections are uniformly biased, the QD ES begins lasing with a threshold of 90 mA, and device has single-mode emission at 1193 nm with a strong side-mode suppression ratio (SMSR) of greater than 40 dB as illustrated in Fig. 2(a). The slope efficiency reported here is 0.12 mW/mA and values as high as 0.24 mW/mA have been reported for LLC-DFB lasers [26]. Although there is no obvious stop band observed in the spectra, the side-modes around 1 nm away from the lasing mode might

#136197 - $15.00 USD Received 6 Oct 2010; revised 26 Nov 2010; accepted 2 Dec 2010; published 8 Dec 2010

be due to the residual index coupling of the chromium metal grating. Figure 2(b), which is the above threshold and wide-span spectra under uniform pumping condition, illustrates the strongly-coupled ES emission peak about 40 nm apart and 30 dB above the broad Fabry-Perot (FP) GS peak.

The κ-value, or the coupling coefficient, is an important design parameter in evaluating the performance of any type of DFB laser. The complex coupling coefficient is described by:

$$\kappa = \kappa_{index} + i\kappa_{gain} = \tilde{\kappa} e^{i\theta},$$

where κ_{index} and κ_{gain} are the index coupling and gain coupling coefficients, respectively. The mixture of index and gain coupling is described by the phase θ at a given coupling strength $\tilde{\kappa}L$, L being the cavity length. The previous methods used for calculating the coupling coefficient in conventional DFB structures with embedded gratings involve approximations which are no longer valid in RWG LLC-DFB structures. Therefore in this paper an improved computer-based program called LAPAREX (Laser Parameter Extraction) developed by T. Nakura *et al.* at the University of Tokyo was used to predict the κ-value of the device under investigation [27]. This program enables predictive calculation of the coupling coefficient for both the gain and index-coupled DFB structures through numerical least-squares-fitting of the measured sub-threshold spectrum with a theoretical sub-threshold fitting algorithm. Least-squares-fitting of the sub-threshold spectra measured from a 1 mm long and two-section QD LLC-DFB laser predicts a gain coupling coefficient value of $\kappa_{gain} = -5.2$ to -3.2 cm^{-1} as the bias current varies from 60 mA to 70 mA, respectively. The negative sign indicates anti-phase complex coupling. Extracted values of the index coupling coefficient shows that this parameter remains relatively unchanged at $\kappa_{index} = 11.5$ to 12.3 cm^{-1} as the bias current changes in the same range mentioned above. The error analyses for the coupling coefficient values are evaluated based on a one standard deviation confidence interval, and are observed to be less than 7% of the extracted values.

3. Generation of two-color emission through asymmetric pumping

Figure 3 illustrates the optical spectrum of the two-section DFB under uniform and asymmetric bias conditions. It is shown that under asymmetric pumping conditions, where the two- sections were biased at 40 mA and 60 mA, respectively, the powers between the GS and ES modes can be equalized. This phenomenon is mainly attributed to the unique carrier dynamics of the QD active gain medium that provides an ES emission close to the GS level. In addition, the inhomogeneous broadening provided by the QD media is crucial towards achieving the two-color emission in a controllable manner.

As opposed to thin-film QW materials, which are homogeneously broadened, the QD media has a wide spectral bandwidth as a result of an inhomogeneously broadened gain in these materials due to QD size dispersion [28]. Although the variation in dot size is normally an unwanted reality, such broadening, which is significant in QD-based materials, can be leveraged to our benefit and allows for GS excitation. When the two sections are biased asymmetrically, the non-uniform distribution of the carriers shifts the refractive index in the active medium which accordingly alters the contribution of the loss/gain mechanism to the ES level provided by the distributed Bragg reflectors. This result also indicates that the total carrier density is not clamped above the threshold, which again can be explained by inhomogeneity of the gain broadening in QDs [23]. Therefore, the excitation of the GS can be

#136197 - $15.00 USD Received 6 Oct 2010; revised 26 Nov 2010; accepted 2 Dec 2010; published 8 Dec 2010

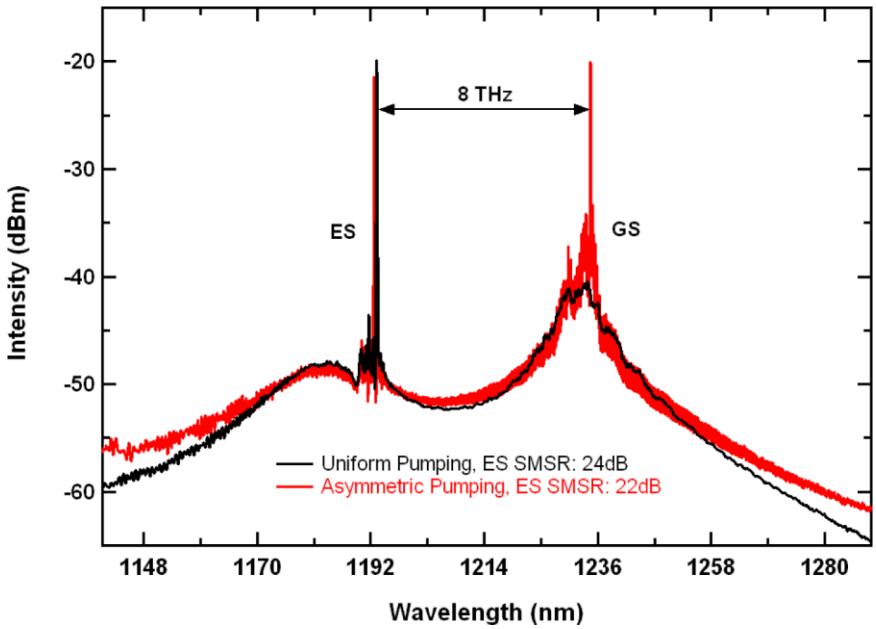

Fig. 3. Wide-span spectra of the QD DFB laser under uniform and asymmetric bias conditions. Under asymmetric pumping, the SMSR for the GS emission is 14 dB.

realized by enforcing the non-uniform distribution of carriers and simultaneously taking advantage of the inhomogeneous gain broadening in QD active media. As a result, a two-color laser with, in this case, an 8 THz difference frequency is realized by combining the benefits of a stable ES-coupled emission peak originating from the distributed Bragg reflector mechanism, the inhomogeneous broadening provided by the QD media, and the asymmetric pumping configuration of the two-section laser diode.

It is important to note that depending on the significance of the inhomogeneous broadening in the nanostructure material under consideration, the frequency difference between the two laser modes can be further tuned to the desired value. For instance, the inhomogeneous broadening in the InAs/GaAs QD laser systems is typically around 40 meV to 50 meV, yet for InAs/InP QD based material it can be as large as 70 meV at room temperature [29]. As a result, a smaller energy separation of ~30 meV between the GS and the ES emissions and consequently smaller difference frequency can be obtained in the InAs/InP material system as opposed to the InAs/GaAs QD materials which have a larger GS and ES energy separation of ~70 meV. Therefore when choosing the appropriate material system for the THz generation source, the magnitude of the inhomogeneous broadening which is a unique signature of the nanostructures can be further taken into the account as an alternative design consideration.

4. Generation of two-color emission through applying external optical feedback

Remarkably, it was demonstrated that under uniform bias condition, the external optical feedback can trigger the GS emission while the excited state remains unchanged. Figure 4 shows the optical spectra measured at 110 mA under uniform pumping in the presence of external optical feedback. The experimental setup used to provide optical feedback to the laser was based on a four-port Polarization-Maintained (PM), 50/50 fiber coupler as schematically illustrated in Fig. 5. The DFB laser output light was injected into port 1 of the coupler using a

#136197 - $15.00 USD Received 6 Oct 2010; revised 26 Nov 2010; accepted 2 Dec 2010; published 8 Dec 2010

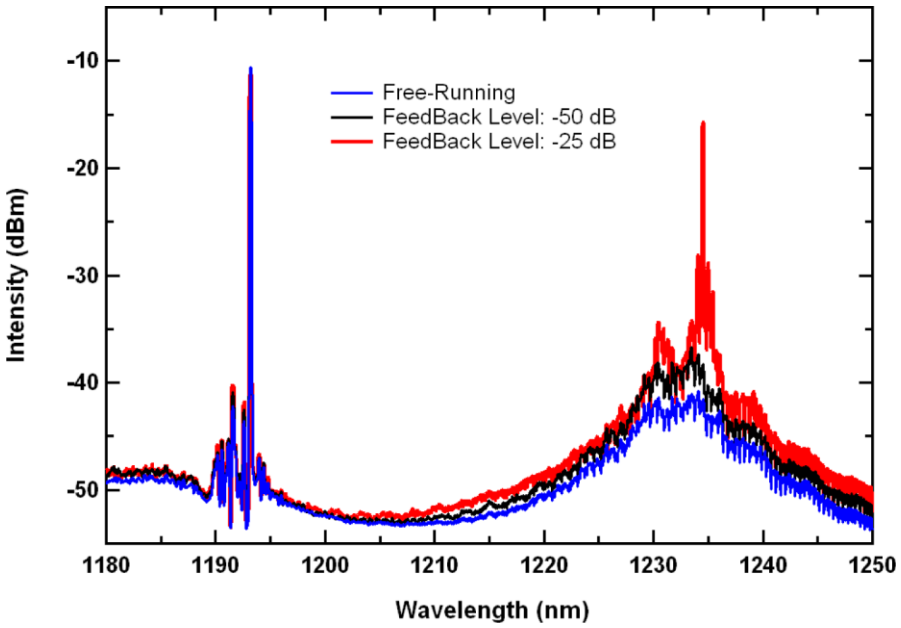

Fig. 4. Broad optical spectra at uniform bias of 110 mA under free-running (no feedback) and external optical feedback level ranges from −50 dB to −25 dB.

PM lensed fiber. The optical feedback was created by an external cavity through a high-reflectivity coated fiber connected to port 2 of the coupler. The applied external feedback level was controlled via a fiber-based variable optical attenuator (VOA) and its value was determined by measuring the output power at port 4. The impact of the external optical feedback on the above threshold spectra was analyzed at port 3 of the fiber coupler via an optical spectrum analyzer (OSA) with a frequency resolution of 2.1 GHz. An optical polarization controller (PC) unit was used to adjust the external feedback beam polarization to be identical to that of the emitted light to maximize the feedback effects. In order to enforce the mode stability, the two-section DFB device was epoxy-mounted on a heat sink and the temperature was maintained at 20 °C. The coupling loss was calculated to be about 4 dB and was carefully monitored and kept constant throughout the entire measurement. Figure 4 shows

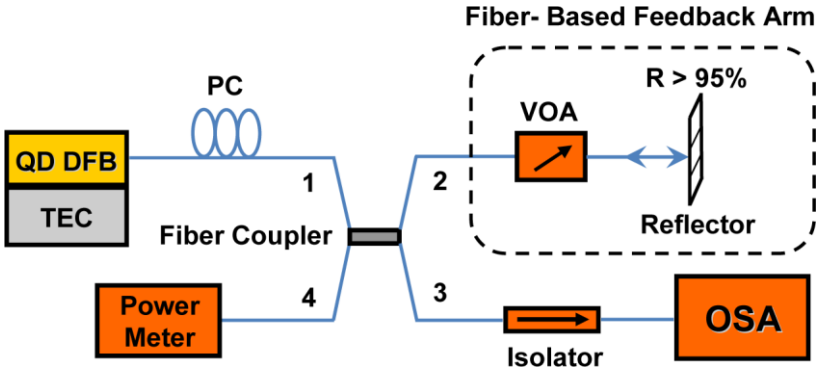

Fig. 5. Schematic diagram of the experimental optical feedback setup.

that as the feedback level is increased from the lowest value (−50 dB) to the highest (−25 dB), the GS FP emission is enhanced and narrowed. Most notably, optical feedback does not affect the ES DFB emission peak located at 1193 nm. The lasing peak is similar to the solitary laser and remains stable even under the strongest feedback level. This robustness of the ES

#136197 - $15.00 USD Received 6 Oct 2010; revised 26 Nov 2010; accepted 2 Dec 2010; published 8 Dec 2010

emission is attributed to the existence of a larger photon density in the cavity provided by the ES coupling through the absorptive metal grating. Similar to the case of asymmetric bias configuration in the two-section QD DFB, the inhomogeneous broadening provided by the QD media helps to reach the two-color emission. Such a broadening when properly combined with external optical feedback permits the excitation and narrowing of the GS emission.

It is important to note that no significant evidence of linewidth broadening or coherence collapse was observed in the ES mode over the entire range of applied feedback levels. This finding confirms that the ES emission on the QD DFB is less sensitive to external reflections as was recently demonstrated in similar QD material system [30]. Such a solid feedback resistivity might be due to the smaller value of the linewidth enhancement factor in the ES emission which is expected to assist in improving the laser's stability under the influence of external optical feedback [31,32].

5. Conclusion

Motivated by the need for compact and low-cost THz sources, two-color operation was demonstrated from a single, two-section QD DFB laser source. An 8 THz mode frequency difference was realized by applying either asymmetric current bias or external optical feedback excitation in a two-section QD LLC-DFB with a stable ES-coupled emission. In order to evaluate the absorptive grating coupling strength of the DFB device under investigation, the values of the gain and index coupling coefficients were determined using the numerical least-squares-fitting method of the sub-threshold spectra. The extracted values for the gain coupling coefficient from least-squares-fitting method was found to be between –5.2 to –3.2 cm^{-1} as the bias current was increased from 60 mA to 70 mA, respectively. It was also shown that the index coupling coefficient remains relatively constant at 11.5 to 12.3 cm^{-1} for the same bias range.

Regarding the demonstration of two-color operation, it was found that when the DFB laser is biased above threshold, the ES emission can be relatively stable while the GS emission is excited and narrowed via either asymmetric pumping of the two-sections or by applying external feedback. This result is only possible in a QD optical media that is inhomogeneously broadened unlike QW media that is homogeneously broadened.

In the future, tuning the two-color emission can be realized through separate design considerations such as choosing a different nanostructure material system with a desired magnitude of inhomogeneous broadening. Furthermore, simultaneous combination of the two methods of asymmetric pumping and optical feedback might be beneficial toward stabilizing and purifying the overall operation of the two-color emission. Compared to existing technologies, the approach described here and current chip-scale photo-mixing capabilities have potential to produce a compact and low-cost CW THz source for future applications.

Acknowledgments

This work was performed, in part, at the Center for Integrated Nanotechnologies, a U.S. Department of Energy, Office of Basic Energy Sciences user facility at Los Alamos National Laboratory (Contract DE-AC52-06NA25396) and Sandia National Laboratories (Contract DE-AC04-94AL85000). This work was also supported by the Air Force Research Laboratory and Air Force Office of Scientific Research under Grant Numbers FA8750-06-1-0085 and FA9550-10-1-0276, respectively. The authors wish to thank Dr. Hui Su for valuable discussions on the use of LAPAREX.

#136197 - $15.00 USD Received 6 Oct 2010; revised 26 Nov 2010; accepted 2 Dec 2010; published 8 Dec 2010